Stochastic and Deterministic Component in Limited Area Model Downscaling

Leo Separovic, Ramon de Elia* and René Laprise
Département des Sciences de la Terre et de l'Atmosphère, Université du Quebec à Montréal
and *Consortium Ouranos

1. Introduction

Limited Area Models (LAMs) have been shown capable to create small-scale features despite the fact of being nested and initialized with coarse resolution Global Circulation Models (GCM) or global analyses. Based on an ensemble of LAM integrations, which differ only in atmospheric and land-surface Initial Conditions (IC), it has been shown that simulations generated by the same set of Lateral Boundary Conditions (LBC) stay partially correlated, regardless of the integration time, unlike the case for global models. The scale analysis of mean square difference between members of an ensemble, performed by de Elia et al. (2002), suggests that the correlation asymptotes to values greater or equal than zero, varying with length scale. For small scales, the asymptotic value is close to zero, while for large scales, driven by LBC, the asymptotic value is close to 1.

In this context, the ability of LAMs to serve as 'intelligent' interpolators of the driving fields is determined by the LAM's capacity to provide not only meaningful information regarding small-scale structures, but, also, that this information be independent of small perturbations in IC. In this study we perform a scale analysis of the ensemble mean of an ensemble of LAM simulations. We will consider the ensemble average as the part of the LAM's solution that is insensitive to small perturbations in IC and thus determined only by LBC. As this part is not affected by internal variability it will be thought of as a deterministic component. The part dependent on IC will be thought of as a stochastic component.

2. Experimental Set-up

The Canadian Regional Climate Model (CRCM), described by Caya & Laprise, (1999) - with 45km horizontal grid spacing (true at 60°N), 18 levels in the vertical, 120x120 domain, centered over Montréal, Canada - was employed to produce 20 three-month simulations for June, July & August 1993 (for further details see Alexandru et al., 2006). The CRCM was nested within regridded coarse (T62) NCEP reanalyses, with updating frequency of 1 per 6hrs. All 20 simulations were generated using identical LBC and ocean surface, differing only in the IC used for the atmospheric and land-surface fields. Each simulation was initialized with a 24hrs time lag, the first one starting on the 1st May 1993 at 00GMT, and the last one on the 20th May at 00GMT – allowing at least 10 days spin-up to assure that internal variability is fully developed during the period of interest. The nesting technique employed here was derived from that proposed by Davis (1977). The domain size was chosen to be neither too small, which could disable small-scale creation (Leduc and Laprise, 2006), nor too large, which could significantly deviate large scales from driving fields (Miguez-Macho et al, 2004). No large-scale nudging was applied.

The 2D spectral variances for selected pressure levels were calculated using Discrete Cosine Transform (DCT), firstly employed for NWP purposes by Denis et al. (2002). The variances were then binned into specific bands of 2D wave number intensity, and, thus, expressed as simple functions of 1D spatial scale.

3. Methodology and Results

Let $\vartheta(\psi_m)$ be the 1D spectral variance of a field ψ_m defined on the LAM grid, where $1 \le m \le M$ denotes the member of the ensemble, and let [ ] denotes the ensemble average over all M simulations. We define the average spectral variance, V, as a mean of M spectral variances computed for each of the members of the ensemble. Thus, we can write:

$$V(k,p,t) \equiv \left[\vartheta(\psi)\right]. \qquad (1)$$

The spectral variance of the ensemble mean is given by

$$V_{ENS}(k,p,t) \equiv \vartheta\left(\left[\psi\right]\right), \qquad (2)$$

and, finally, the spectral variance of regridded NCEP reanalyses by

$$V_{OBS}(k,p,t) \equiv \vartheta\left(\psi_{OBS}\right). \qquad (3)$$

Here k represents the 1D wave number, p is the pressure level, and t is integration time. If, at any length scale, individual runs have no spread among them, then the variances given by (1) and (2) become identical. Furthermore, at large-scales, where no spread is expected to appear, any difference between variances (2) and (3) is undesirable, because it indicates that the LAM does not simulate the observed amount of variance. On the contrary, at small-scales, the positive difference between V_{ENS} and V_{OBS} implies that the downscaled information contains a deterministic part. In particular, for small scales, unresolved by the driving fields, a difference between

variances (1) and (2) indicates the stochastic part of the downscaled variance, while a difference between variances (2) and (3) indicates the component independent of IC.

The variances given by equations (1), (2), and (3), for geopotential at 925hPa, sampled every 6 hrs and averaged over 3 summer months of 1993 are shown in Figure 1. It can be seen that for the largest resolved scales there is a slight excess of variance in both the individual runs and their ensemble average relative to the reanalyses. We notice that this excess was detected only under the 600hPa-level; in the upper part of the troposphere we found a slight lack of variance at those scales (not shown). For wave numbers larger then 5 (~1100km) - the effective resolution of reanalyses - the variance of reanalyses should be equal zero as those scales are not represented in the driving fields. Due to the regridding noise and Gibbs effect of the DCT this is not the case. A difference between V and V_{ENS} appears for wave numbers larger then 10 (~500km), as a consequence of spread among the runs. Furthermore, V_{ENS} has a noticeably higher value then V_{OBS}, for all wave numbers larger then 5, implying that a part of the downscaled variance is due to small-scale structures common to all members of the ensemble. It is worth noting that similar behaviour was found at all levels, with a decrease of difference between V_{ENS} and V_{OBS} with height, (not shown).

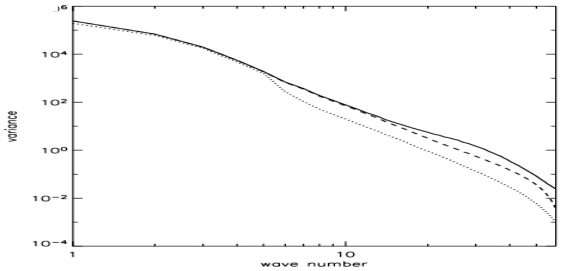

FIG. 1. Spectral variance of geopotential at 925hPa: *full line* - average spectral variance of individual runs, equation (1); *dashed line* - spectral variance of ensemble mean, equation (2); *dotted line* - spectral variance of reanalyses, equation (3). The variances were sampled every 6 hours and the sample mean for 3-month long period is presented.

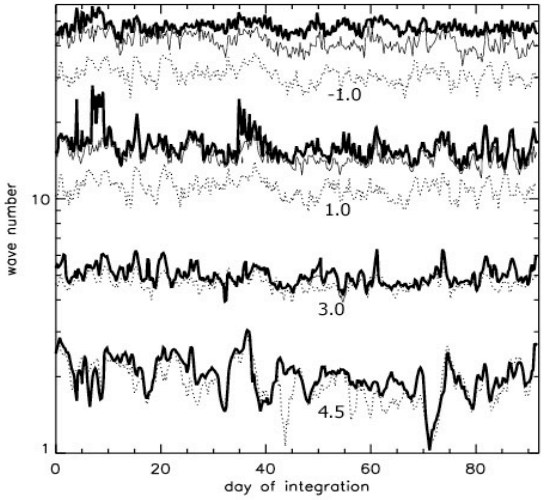

FIG. 2. Logarithm of spectral variance of geopotential field at 925hPa: *full thick line* - average spectral variance of individual run, equation (1); *full thin line* - spectral variance of ensemble mean, equation (2); *thin dotted line* - spectral variance of reanalyses, equation (3). Isolines are drawn for four different values: -1.0, 1.0, 3.0, and 4.5.

The scale distribution of the temporal evolution of variances given by equations (1), (2), and (3) is shown in Figure 2. It can be seen that, for the largest resolved scales of thousands of kms (isolines of 4.5), the excess of the simulated variance relative to the reanalyses is not systematic but intermittent during periods of few days, thus contributing to the temporal mean in Figure 1. The isolines of −1.0 and 1.0, which represent the behaviour of non-driven small-scales, show that the difference between V_{ENS} and V_{OBS} is present at all times. On the contrary, the difference between V and V_{ENS} exhibits more complicated behaviour, indicating that the intensity of spread pulsates according to weather pattern. We notice that the isolines of 3.0 exhibit little spread, except around day 48, when the internal variability seems to penetrate inside driven scales. This is clearly visible on the geopotential maps of that day.

4. Conclusion

Our results suggest that the downscaled information provided by the CRCM is partially determined by the boundary conditions and partially of stochastic nature (dependent on small, uncontrollable changes in IC). Hence, the value added by dynamical downscaling has to be sought in both components. It is worth noting that the deterministic component is stronger near the surface. The results also show that the large-scale information is sometimes modified inside the domain, and that this tends to happen in all individual runs in the same manner. This seems to suggest that the CRCM is unable to reproduce some of the large-scale weather patterns provided at the boundaries.

References:

Alexandru A., R. de Elia, and R. Laprise, 2006, Geographical distribution of internal variability in regional downscaling, the same volume.

Caya D., and R. Laprise, 1999, A semi-implicit semi-Lagrangian regional climate model: The Canadian RCM, *Mon.Wea.Rev.,* 127, 341-362.

Davies, H.C., and R.E. Turner, 1977, Updating prediction model by dynamical relaxation: An examination of the technique, *Quart.J. Roy.Meteor.Soc.,* 103,225-245.

De Elia R., and R. Laprise, 2002, Forecasting skill limits od nested, LAMs: A perfect model approach, *Mon.Wea.Rev*., 130, 2006-2023.

Denis B., J. Côté, and R. Laprise, 2002a, Spectral decomposition of two-dimensional fields on limited-area domains using the discrete cosine transform, *Mon.Wea.Rev.,* 130, 1812-1829.

Leduc M. and R.Laprise, 2006, CRCM sensitivity to domain size, the same volume.

Miguez-Macho G., G.L. Stenchikov, and A. Robock, 2004, Spectral nudging to eliminate the effects of omain position geometry in regional climate model simulations, *J.Geophys.Res.,* 109, D13104, doi: 10.1029 /2003JD004495